Quantifying the role of stochasticity in incomplete penetrance of Hirschsprung Disease

Benjamin J. Binder[a,*], Kerry A. Landman[b], Donald F. Newgreen[c], Joshua V. Ross[a]

[a]*School of Mathematical Sciences, University of Adelaide, South Australia 5005, Australia*
[b]*Department of Mathematics and Statistics, University of Melbourne, Victoria 3010, Australia*
[c]*Murdoch Childrens Research Institute, Royal Children's Hospital, Parkville, Victoria 3052 Australia.*

Abstract

In Hirschsprung Disease the enteric nervous system is absent from a variable segment of the distal bowel due to incomplete proximal-to-distal colonization of the elongating embryonic gut by migrating and proliferating neural crest precursor cells. Genetic causes of this disease are many and most are classed as dominant mutations. However not all individuals with the same mutation show the disease; this is termed incomplete penetrance. This incomplete penetrance extends even to discordancy in monozygotic (identical) twins. We develop a continuous-time Markov chain model that approximates a continuous-time one-dimensional stochastic agent-based model of the colonization process. The probability mass function for the most distally-advanced agent is obtained for the agent-based model and its approximation, and they compare extremely well. These results confirm that the neural crest agent proliferation is the most important parameter in determining success of full colonization. Furthermore, the results suggest that when the neural crest agent proliferation and migration rates are sufficiently large to simulate the normal genotype (i.e., in the absence of the Hirschsprung Disease mutation), small perturbation of these rates leads to only small changes in colonization rate, but almost always resulting in successful colonization. A different outcome occurs with lowered neural crest agent proliferation or migration rate (but with elongation of the gut unchanged from normal) to simulate the effect of a Hirschsprung Disease mutation. For this case, success or failure of colonization is probabilistic, equivalent to incomplete penetrance. This idea places limits on the predictability of this disease even if a full genetic and epigenetic description could be obtained.

Keywords: Hirschsprung disease, enteric nervous system, Markov chain model, agent-based model

1. Introduction

Hirschsprung Disease is a serious and quite common developmental defect (about 1/5000 live births) in which the enteric nervous system (ENS) is absent from the distal intestine, resulting in a regional failure of peristalsis (Newgreen & Young 2002a). The ENS derives from a small number of hindbrain neural crest (NC) cells which colonize the gut in a proximal-to-distal invasion of cells migrating within the intestinal wall. NC cells normally complete colonization of the distal colon at seven weeks gestation (Fu *et al.* 2004). Completion of colonization is made more difficult by the simultaneous elongation of the intestine itself (Binder *et al.* 2008; Binder & Landman 2009). This mode of ENS formation is conserved among vertebrates, which also exhibit Hirschsprung-like defects (Newgreen & Young 2002a; Newgreen & Young 2002b). In rodent models the cause of this defect is generally failure to complete proximal-to-distal colonization. Because ENS formation in humans descriptively and genetically resembles that in rodents, it is presumed in most cases to arise in humans as a defect in early colonization, with the critical period prior to seven weeks gestation.

The diagnosis of Hirschsprung Disease is unequivocal, but its origins are complex, with predisposing mutations in many genes (Amiel *et al.* 2008; Burzynsk *et al.* 2009). Individuals with identified mutations in Hirschsprung

*Tel: 61 883133244. Email: benjamin.binder@adelaide.edu.au

Disease genes, for example mutation of one copy of the gene RET, may not show the disease while others show a variable length of affected intestine. This incomplete penetrance and variable severity (lumped here as incomplete penetrance) are apparently stochastic phenotypic variations exhibited after defined gene mutations. These surprising and apparently chance-based variations have been discussed since the mid-1920s with their biology receiving renewed interest (Oates 2011).

The most puzzling aspect of incomplete penetrance occurs when monozygotic (identical) twins are discordant, and Hirschsprung Disease illustrates this (Hannon & Boston 1988; Moore *et al.* 1979; Siplovich *et al.* 1983). For example, in a description of over 130 cases of Hirschsprung Disease, Jung (Jung 1995) noted three sets of monozygotic twins, all of whom were discordant. Moreover, in another set of monozygotic twins, Hirschsprung Disease occurred with sensorineural deafness. This association (Waardenburg Syndrome type 4 or Waardenburg-Shah syndrome) arises from mutations in genes (SOX10, EDNRB or EDN3) that control development of both the ENS and the auditory system. Both twins were deaf, showing both had the mutation, but only one showed Hirschsprung Disease (Sarioglu *et al.* 2000). Similar variability of colonization or incomplete penetrance has also been observed with inbred mouse models (Uesaka *et al.* 2008).

Most explanations of incomplete penetrance in genetically identical individuals are made by assuming differences in gene expression between affected and unaffected individuals. We suggest here a novel explanation of incomplete penetrance in Hirschsprung Disease based on (typical) stochastic cell behavior, amplified by disease-causing mutations. Intuitively, for a high NC migration rate we would expect colonization to be always successful, whereas at a low NC migration rate we would expect colonization to be always unsuccessful. This raises the following question: on ramping down the NC cell motility and/or proliferation rate(s), but maintaining the normal elongation of the intestine, does the outcome at the level of the whole system suddenly switch from successful to unsuccessful colonization at some point. Since the stochasticity acting here does so at the level of each single cell, and each cell is equivalent to any other cell, and the system has very many cells, one might suggest a very predictable switch-style outcome at the system level. Alternatively, does colonization success degrade gradually and probabilistically? This would mean that there may exist identical starting conditions with a variable success in colonization, hence allowing for incomplete penetrance (see Fig. 1).

We investigate this by considering two continuous-time one-dimensional Markovian models: one an agent-based model as previously used in this area, and the other an approximating model. The agent-based (cellular automata) model simulates the unidirectional proximal-to-distal invasion of NC cells within the growing gut tissue. This is the continuous-time 1-D analogue of the discrete-time 2-D agent-based model for the mechanisms of NC cell proliferation and motility, and gut cell proliferation (Binder *et al.* 2008; Binder & Landman 2009; Simpson *et al.* 2007; Zhang *et al.* 2010). Although the probability distribution of the state of the agent-based model is determined by a set of ordinary differential equations, the size of this system makes it impractical to solve. We therefore derive a second model which is a Markov chain approximation to quantify the variability of the NC invasion front, providing a measure of colonization success.

The approximation is validated by comparison with averaged simulation data from the agent-based model of the overall process, demonstrating a high level of accuracy across a wide range of parameter space. The results suggest that the variability in colonization, as observed in the case of discordancy between genetically similar monozygotic twins, can be attributed to the stochastic interactions of the cellular mechanisms.

2. Agent-based model

We consider a continuous-time one-dimensional discrete-state agent-based model to simulate the NC colonization. All quantities and variables are non-dimensional. The domain (gut tissue) is a single row of lattice sites whose positions are located at the discrete integer points $x = 1, 2, \ldots, L(t)$, where $L(t)$ is the length of the domain that elongates with time t. Each lattice site of the domain can be either occupied by a single NC agent or unoccupied. The total number of NC agents at any given time is $N(t) \in \{1, 2, \ldots, L(t)\}$. The model update rules, similar to those described previously (Binder *et al.* 2008; Binder & Landman 2009) for domain growth, NC agent motility and NC agent proliferation events are shown in Fig. 2. If the target site is occupied for any NC motility or proliferation event, then that event is aborted. These events are volume exclusion processes (Chowdhury *et al.* 2005; Simpson *et al.* 2009). Note that if the chosen lattice site is occupied by an NC agent in the case of a domain growth event, then the NC agent is transported to the right with the moving lattice site.

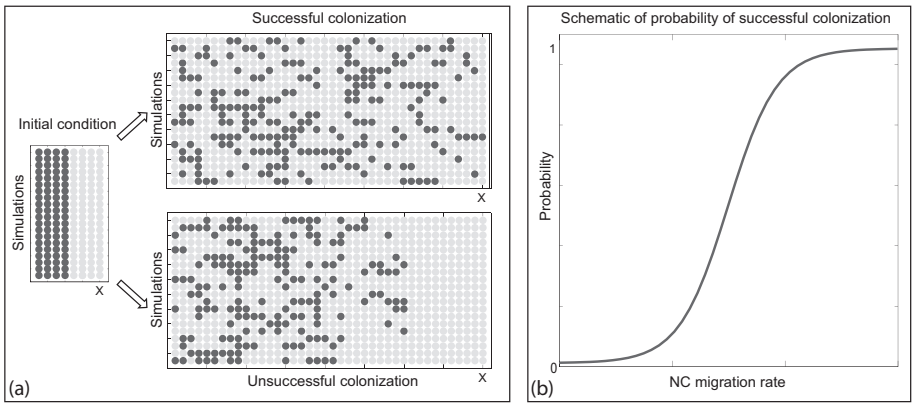

Figure 1: Successful and unsuccessful outcomes of the agent-based model and schematic diagram of probability of successful outcomes. (a) Agents, representing NC cells (dark grey), initially occupy the left-hand end of the domain, representing the gut mesoderm cells (light grey). The gut is elongating by progressive cell division, modelled by a uniformly growing domain. The NC agents are dividing and are allowed to move in the horizontal direction only. For some simulations the colonization may be classified as successful, while in other simulations under identical conditions the colonization is classified as unsuccessful. This difference in outcomes arises from the stochastic nature of the division and movement processes. (b) The schematic diagram shows the probability of successful colonization as a function of the NC migration rate.

The model is updated in continuous-time (Gillespie 1977) with domain growth rate, λ_g, NC agent motility rate λ_m and NC proliferation rate λ_p. We define the propensity function as $\lambda = (\lambda_m + \lambda_p)N(t) + \lambda_g L(t)$, giving the total rate at which events occur at time t. Random numbers are drawn from the exponential distribution and standard discrete uniform distribution as $E[\lambda^{-1}]$ and $U[0, 1]$, respectively. The algorithm then proceeds as follows, being terminated at either a maximum chosen time $t_f > 0$ or maximum chosen domain length $L_f > L(0)$.

Step 1: Calculate the propensity function λ given the current state, and update the time with $t := t + E[\lambda^{-1}]$. If $t < t_f$ (or alternatively $L(t) < L_f$) go to Step 2; else stop.

Step 2: Generate a random number $R = \lambda U[0, 1]$.

Step 3: Decide which type of event to perform. If $R < \lambda_m N(t)$ then attempt to perform a NC motility event. If $\lambda_m N(t) \leq R < (\lambda_m + \lambda_p)N(t)$ then attempt to perform a NC proliferation event. If $R \geq (\lambda_m + \lambda_p)N(t)$ then perform a domain growth event. Update the state as appropriate.

Step 4: If $t < t_f$ (or alternatively $L(t) < L_f$) repeat steps 1–3; else stop.

We initialize a simulation by populating all the lattice sites to the left of and including the site z_0, where $1 \leq z_0 \leq L(0)$, and then record the position of the rightmost NC agent at later times. This provides a measure for the NC invasion front. Shown in Fig. 1(a) are two sets of simulations (successful and unsuccessful) that were terminated when $L_f = 40$, with $z_0 = 4$, $L(0) = 8$, $\lambda_p = 0.4$, $\lambda_m = 1.0$ and $\lambda_g = 0.40$.

To quantify the success of the colonization we record the counts (number of occurrences) of the positions $z(t)$, where $z_0 \leq z(t) \leq L(t)$ for $t > 0$ and $z(0) = z_0$, of the rightmost or leading agents from M realisations. Dividing the counts by the number of simulations M then produces an estimated probability mass function (PMF) $P(z)$, for the position of the rightmost NC agent or invasion front. Typical PMFs are shown in Figs. 3 and 4 (light grey). We delay the discussion of these curves to Section 4.

3. Markov chain approximation

We now consider an approximating Markov chain model of the process of cell invasion and tissue growth. We define the model and then discuss the evaluation of the main quantity of interest, the PMF of rightmost NC agent.

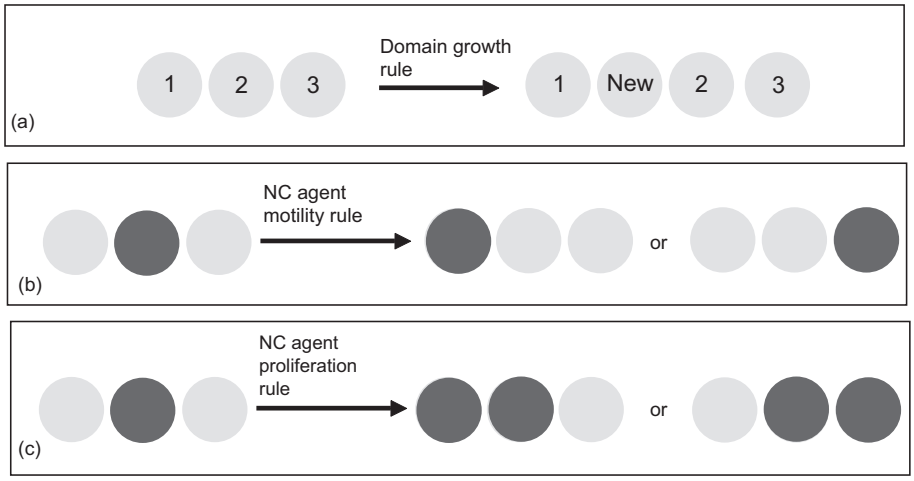

Figure 2: Agent-based mechanisms, domain agents (light grey) and NC agents (dark grey). (a) Domain growth rule. (b) NC agent motility rule. The NC agent can move to one of the two configurations shown with equal probability. (c) NC agent proliferation rule. The mother NC agent divides into two daughter agents. After mitotic division two possible configurations can occur with equal probability.

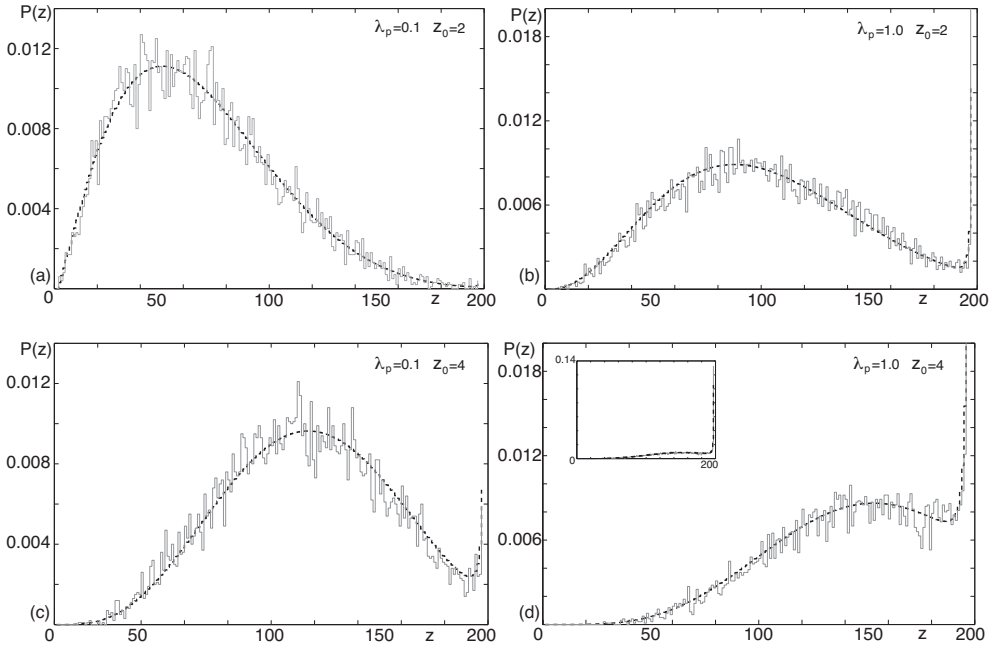

Figure 3: Comparison of PMFs for the position of the rightmost (leading) NC agent generated by the agent-based model and the Markov chain approximation for various values of proliferation rate λ_p and initial position of the rightmost agent z_0. The agent-based model results (grey) are generated from $M = 10000$ simulations with a final length $L_f = 197$ and average final time $\bar{t} = 8$; $L(0) = 8$, $\lambda_m = 1.0$ and $\lambda_g = 0.4$. The Markov chain approximation is also shown (the black broken curves). (a) Initial population $x_0 = 2$; $\lambda_p = 0.1$. (b) Initial population $z_0 = 2$; $\lambda_p = 1.0$. (c) Initial population $z_0 = 4$; $\lambda_p = 0.1$. (d) Initial population $z_0 = 4$; $\lambda_p = 1.0$. The inset shows the complete data.

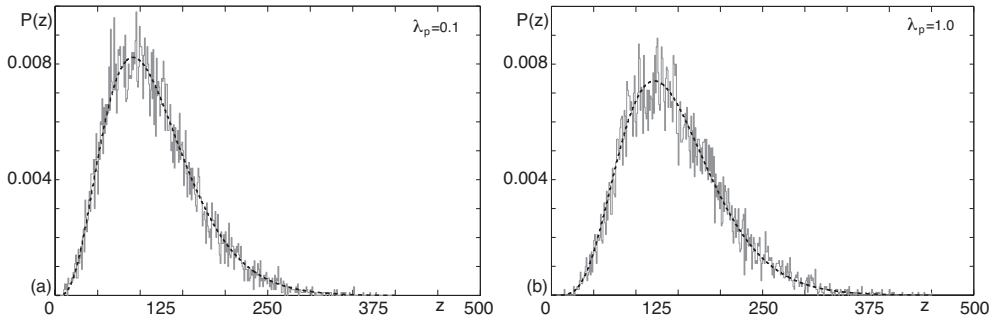

Figure 4: Comparison of PMFs generated by the agent-based model and the Markov chain approximation for various values of proliferation rate λ_p. The agent-based model results (grey) are generated from $M = 10000$ simulations with a final length time $t_f = 8$ and average final length $\bar{L} = 197$; $L(0) = 8$, $z_0 = 4$, $\lambda_m = 1.0$ and $\lambda_g = 0.4$. The Markov chain approximation is also shown (the black broken curves). (a) $\lambda_p = 0.1$. (b) $\lambda_p = 1.0$.

Our approximating model is a trivariate continuous-time Markov chain, where the variables are $z(t)$, the position of the rightmost occupied site, $n(t)$, the number of sites occupied to the left of the rightmost occupied site, and $l(t)$, the length of tissue, at time t.

Since agents cannot jump over each other in the model, the agent in the rightmost position will be the same agent or a daughter of the agent in the rightmost position for all t. This rightmost agent can move to the right, via motility and proliferation, uninhibited provided it is currently not occupying the last site in the tissue, and hence requires no approximation. However, an approximation is required when modelling motility and proliferation of this agent when moving to the left, and for the motility and proliferation of the other $n(t)$ agents, as we do not (typically) know the exact configuration of the agents and hence the exact probability the sites will be vacant, and hence accessible for movement and proliferation events. Tissue growth can also be modelled without approximation; however, its impact on the precise configuration of the $n(t)$ agents is unknown.

The dynamics (non-zero transition rates) of our model are described by six changes of state, detailed below.

$$
\begin{aligned}
&(i) && (z,n,l) \to (z+1,n,l) && \text{at rate} && \frac{\lambda_m}{2}1_{\{z<l\}}\\
&(ii) && (z,n,l) \to (z+1,n+1,l) && \text{at rate} && \frac{\lambda_p}{2}1_{\{z<l\}}\\
&(iii) && (z,n,l) \to (z-1,n,l) && \text{at rate} && \frac{\lambda_m}{2}\left(\frac{z-n-1}{z-1}\right)\\
&(iv) && (z,n,l) \to (z,n+1,l) && \text{at rate} && \frac{\lambda_p}{2}\left(\frac{z-n-1}{z-1}+nb(z,n)\right)\\
&(v) && (z,n,l) \to (z+1,n,l+1) && \text{at rate} && \lambda_g z\\
&(vi) && (z,n,l) \to (z,n,l+1) && \text{at rate} && \lambda_g(l-z).
\end{aligned}
$$

Here the notation $1_{\{z<l\}}$ is unity if $z < l$ and zero otherwise, and $b(z,n)/2 = (z-n-1)/[2(z-1)-n]$. Transition (i) describes a motility event of the rightmost agent to its immediate right (to $z+1$), while (ii) describes a proliferation event of the rightmost agent, where a daughter is placed to its immediate right ($z+1$). Only the second event changes the total number of agents to the left of the rightmost agent, and the length of the domain remains unchanged. In both these cases, we know that $z+1$ is unoccupied, so the transitions automatically occur. Transitions (v) and (vi) represent domain growth to the left and right of the rightmost agent respectively.

Transitions (iii) and (iv) involve additional terms which are approximations requiring explanation. The first, (iii), represents a move of the rightmost agent to its immediate left (to $z-1$) with no change in the number of agents. The

second, (iv), represents a proliferation event of the rightmost agent at z to its immediate left $(z-1)$ or a proliferation event of any of the n agents to the left of z, ensuring that the rightmost agent remains at z, but the total number of agents increases by unity. A movement or proliferation event of the rightmost agent can only occur if the site at $z-1$ is unoccupied, so depends on volume exclusion. We therefore need to modify the attempted transition rate (namely $\lambda_m/2$ in (iii) and $\lambda_p/2$ in (iv)) by the probability of site $z-1$ being vacant. If we assume that the occupied sites are uniformly distributed between sites 1 and the rightmost occupied site z, then the factor $(z-n-1)/(z-1)$ is the probability of the site to the left of the rightmost agent being vacant (since it is just the number of vacant sites to the left of the rightmost agent divided by the total number of sites to its left). In (iv), we also need to account for proliferation events of any agent to the left of z. This occurs at rate $\lambda_p n/2$ times the probability there is a vacant site to one side of the chosen agent. Because one of the mechanisms by which sites become occupied is proliferation, it means it is more likely that occupied sites will be adjacent to each other (rather than just if they had been laid down at random), and hence a proliferating agent is less likely to find a vacant site. As noted, we define $b(z,n)/2 = (z-n-1)/[2(z-1)-n]$ as the approximation for this probability, which accounts for the fact that as the number of agents, n, increases for a fixed number of sites, $z-1$, there must be an decrease in the probability of site vacancy. Since $b(z,n)/2 \leq (z-n-1)/(z-1)$, this function reduces the rate from that which arises under an assumption of uniformly-distributed agents, to account for the mechanism of proliferation which increases the likelihood of agents occupying adjacent sites.

We evaluate the distribution of the state of this approximating Markov chain using `EXPOKIT` (Sidje 1998). From this distribution we may evaluate any quantity of interest, such as the marginal PMF of the position of the rightmost agent shown by the broken curves in Figs. 3 and 4. We discuss these figures and their implications next.

4. Results and Discussion

PMFs of the rightmost NC agent have been generated with the two different stopping criteria (either a final length L_f or a final time t_f is chosen), for various values of the NC proliferation rate λ_p and the initial position of the rightmost agent z_0.

When the colonization process is terminated at a fixed domain length $L_f = 197$, with an average time of simulation $\bar{t} = 8$ (Fig. 3), the effect of increasing both λ_p and z_0 is an increase in colonization success, indicated by the probability distribution of the position of the advancing NC colonization front. The spikes in the PMFs (Figs. 3(b)–(d)) at $L_f = 197$ correspond to NC agents that happened to reach the end of the domain during the simulations and then being transported by the domain growth mechanism.

Alternatively, when the colonization process is terminated at a fixed time $t_f = 8$, with an average final length of domain $\bar{L}_f = 197$ (Figs. 4), we observe that there is a smaller increase in the advancing colonization front (Fig. 4) for the same increase in proliferation rate of that in the fixed final length case (Figs. 3(c)–(d) with the same parameter values). Also noteworthy, the spikes in the PMFs are no longer present in Fig. 4, due to the (large) variability in the final length of the domain.

Moreover, the comparison between the averaged simulation data (light grey curves) and Markov chain approximation (black broken curves) for both sets of results is excellent. Therefore, our approximate Markov chain is a good approximation to the agent-based model.

The accuracy of the Markov chain approximation is further examined by the sum, Q, of marginal probabilities of occupancy $P(z)$:

$$Q = \sum_{z=\lfloor \beta L_f \rfloor}^{L_f} P(z).$$

In Fig. 5 we chose $\beta = 3/4$ for the case where a given L_f is the stopping criteria. The effect of increasing both the NC proliferation and motility rate (λ_p and λ_m respectively), for three values of the gut (domain) growth rate (λ_g) is illustrated. The quantity Q provides a probabilistic indicator of colonization success similar to that shown in the schematic of Fig. 1. Note that as the value of $\beta \to 1^-$, the curves will increase at a less rapid rate.

Comparison between Fig. 5(a) and (b) show that the Q increases more rapidly as the NC agent proliferation rate, λ_p, is increased than when the NC agent motility rate, λ_m, is increased. Indeed the results suggest that increasing the NC proliferation is the most effective way of decreasing the probability of failure to complete colonization (i.e., Hirschsprung Disease), for a fixed or normal gut growth rate.

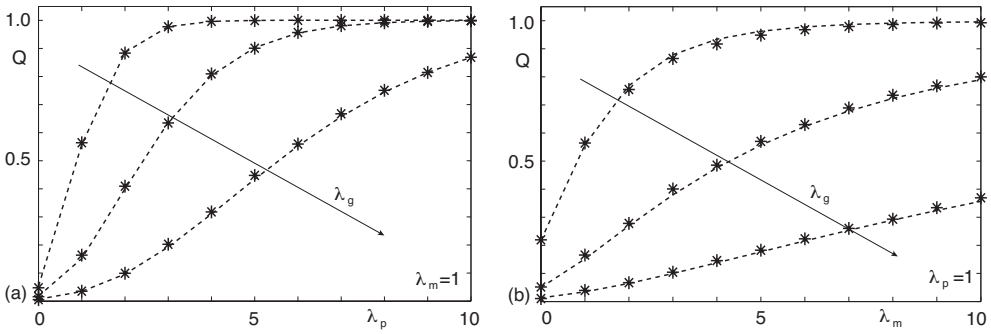

Figure 5: Sum of probabilities Q, in the last 25% of the length of tissue, $L_f = 197$, $L(0) = 8$ and $z_0 = 2$. The arrow indicates the increasing rate of gut growth for the three sets of results, $\lambda_g = \{0.2, 0.4, 0.8\}$. The agent-based model, averaged over $M = 10000$ simulations, (black markers) and the Markov chain approximation (broken curves) are both illustrated. (a) Increasing proliferation rate with fixed motility rate; $\lambda_m = 1$. (b) Increasing motility rate with fixed proliferation rate; $\lambda_p = 1$.

The puzzle of incomplete penetrance of a disease phenotype is usually explained by assuming that, between individuals with the same primary disease-causing mutation, other pre-existing differences occur which determine the difference in disease phenotype. In individuals with different genotypes, this difference in disease expression is assumed to occur mostly because individuals have different alleles of so-called disease modifier genes (Nadeau 2003). Indeed, a number of genes that modify the penetrance of Hirschsprung Disease genes have been described (Wallace & Anderson 2011). In highly inbred animals or monozygotic twins each individual has the same modifier gene variants, yet reduced penetrance disease still occurs. In this case, one assumption is that differences occur even between such closely related individuals in the gestational or post-gestational environment, and this differentially influences gene expression (Khoury *et al.* 1988). The second assumption is that differences in expression of genes that influence the specific phenotype can arise between individuals by somatic genetic or epigenetic mutations. These two effects can interact in a complex way (Gordon *et al.* 2012). In any case, although these genetic differences may arise stochastically, once present they drive the phenotype so that some individuals are affected while others with the same primary disease-causing mutation are not. In theory at least these gene sequence or expression differences, or epigenetic differences, can be discovered by large scale genetic testing (Grundberg *et al.* 2012).

We propose here an additional and fundamentally different mechanism for incomplete penetrance which requires no differences of genes or their expression, or change of environmental conditions. This explanation depends on the rules that govern defined aspects of the behaviour of individual cells having innately stochastic components, in this case their proliferation (Cheeseman *et al.* 2014) and movement (Young *et al.* 2014). This same model could apply to many other incompletely penetrant birth defects, particularly neurocristopathies (Singh *et al.* 2002). This means that in such cases prognostic certainty at an individual level cannot be obtained even if all determinants are known, and adds to the considerable difficulties in risk assessment for diseases with incomplete penetrance (Emery 1986).

To test stochastic causation in experiments is a formidable challenge. The genetically deterministic alternative could be tested in inbred mice with incompletely penetrant Hirschsprung-like phenotype such as these recently produced (Uesaka *et al.* 2008). This could be performed by comparing individuals at the earliest stage when differences in their ENS can be detected. This early stage would be necessary to capture the gene expression signature at or nearest the time when causative developmental genetic mechanisms are acting. Demonstration, for example by microarray technology, that gene expression differences in ENS cells or in cells of their microenvironment occurred between different individuals, and that these correlated with the presence or degree of their Hirschsprung-like phenotype would be consistent with an explanation determined by gene expression levels. This of course would not rule out additional sources of variation. In contrast, failure to demonstrate any such correlated differences would not be consistent with this genetic determinist model, and would allow (but not prove) that the discordancy arises at a level above gene expression, such as we propose. To more directly investigate whether this could be due to the stochasticity of cell behavior, as proposed here, genetic alterations might be made to the rules of cell behaviour. Isolated ENS cells in gut tissue show a random walk which is directionally biased by cell contacts (Young *et al.* 2014). The cell speed could

be preserved while the cells' directional walk probabilities could be altered. One way this could be implemented experimentally is by providing a consistent invariant directional bias by introducing an over-riding chemotactic gradient (Young *et al.* 2001). In addition, the directional response to cell contact could also be manipulated by targeting molecules that control contact inhibition of locomotion (Stramer *et al.* 2013). Both these should lead to a shift of the curve shown in Fig. 1, consistent with the direction of bias.

Acknowledgments

The contributions of Binder, Landman and Newgreen was supported by the National Health and Medical Research Council. The contribution of Ross was supported by an Australian Research Council Future Fellowship (ARC FT130100254). MCRI facilities are supported by the Victorian Governments Operational Infrastructure Support Program.

References

Amiel, J., Sproat-Emison, E., Garcia-Barcelo, M. *et al.* 2008. Hirschsprung disease, associated syndromes and genetics: a review. J. Med. Genet. 45, 1-14.

Binder, B.J., Landman, K.A., Simpson, M.J., Mariani, M., Newgreen, D.F., 2008. Modeling proliferative tissue growth a general approach and an avian case study. Phys. Rev. E 78, 031912.

Binder B.J., Landman, K.A., 2009. Exclusion processes on a growing domain. J. Theor. Biol. 259, 541-551.

Burzynski G., Shepherd I. T., Enomoto H., 2009. Genetic model system studies of the development of the enteric nervous system, gut motility and Hirschsprung's disease. Neurogastroenterol Motil. 21, 113–127.

Cheeseman B.L., Zhang, D., Binder, B.J., Newgreen, D.F, Landman K.A., 2014. Superstars and cell invasion waves: Cell lineage tracing experiments and mathematical analyzes of the developing enteric nervous system. J Royal Soc. Int. 11, 20130815.

Chowdhury, D., Schadschneider, A., Nishinari, K., 2005. Physics of transport and traffic phenomena in biology: from molecular motors and cells to organisms. Phys. Life Rev. 2, 318–352.

Emery A. E. H., 1986. Risk estimation in autosomal dominant disorders with reduced penetrance. J. Med. Genet. 23, 316–318.

Fu M, Tam PK, Sham MH, Lui VC. 2004. Embryonic development of the ganglion plexuses and the concentric layer structure of human gut: a topographical study. Anat Embryol (Berl). 208, 33–41.

Gillespie, D.M., 1977. Exact stochastic simulation of coupled chemical reactions. J. Phys. Chem. 81, 2340–2361.

Gordon, L. *et al.* 2012. Neonatal DNA methylation profile in human twins is specified by a complex interplay between intrauterine environmental and genetic factors, subject to tissue-specific influence. Genome Res 22, 1395–1406.

Grundberg, E, *et al.* 2012. Multiple Tissue Human Expression Resource (MuTHER) Consortium Mapping cis- and trans-regulatory effects across multiple tissues in twins. Nat Genet 44,1084–1089.

Hannon, RJ, Boston VE. 1988. Discordant Hirschsprung's disease in monozygotic twins: a clue to pathogenesis? J Pediatr Surg. 23, 1034-1035.

Jung, P. M., 1995. Hirschsprung disease: one surgeon's experience in one institution. J Pediatr Surg. 30, 646–51.

Khoury, M. J., Flanders, W. D., Beaty, T. H., Optiz, J. M., 1988. Penetrance in the presence of genetic susceptibility to environmental factors. Am J Med Genet 29, 397–403.

Moore, T. C., Landers, D. B., Lachman, R. S., Ament, M. E., 1979. Hirschsprung disease discordant in monozygotic twins: a study of possible environmental factors in the production of colonic aganglionosis. J Pediatr Surg. 14, 158–61.

Nadeau J.H. 2003. Modifier genes and protective alleles in humans and mice. Modifier genes and protective alleles in humans and mice. Curr. Opin. Genet. Dev. 13, 290–295.

Newgreen, D., Young, H. M., 2002a. Enteric nervous system: development and developmental disturbances-part 1. Pediatr Dev Pathol. 5, 224-47.

Newgreen, D., Young, H. M., 2002b. Enteric Nervous System: development and developmental disturbances-Part 2. Pediatr Dev Pathol. 5, 329–49.

Oates, A. C., 2011. What's all the noise about developmental stochasticity? Development. 138, 601-7.

Sarioglu, A., Senocak, M. E., Hicsonmez, A., 2000. Discordant Hirschsprung disease in monozygotic twins with concordant congenital deafness. Eur J Pediatr Surg. 10, 204-6.

Sidje, R. B., 1998. EXPOKIT: A software package for computing matrix exponentials. ACM Trans. Math. Softw., 24, 130–156.

Simpson, M.J., Zhang, D.C., Mariani, M., Landman, K.A., Newgreen, D.F., 2007. Cell proliferation drives neural crest cell invasion of the intestine. Dev. Biol. 302, 553–568.

Simpson, M.J., Landman, K.A., Hughes, B.D., 2009. Multi-species simple exclusion processes. Physica A 388, 399–406.

Singh, S. M., et al. Singh, S.M., Murphy, B., O'Reilly, R., 2002. Monozygotic twins with chromosome 22q11 deletion and discordant phenotypes: updates with an epigenetic hypothesis. J Med Genet 39 e71.

Siplovich, L., Carmi, R., Bar-Ziv, J., Karplus, M., Mares, A. J., 1983. Discordant Hirschsprung disease in monozygotic twins. J Pediatr Surg. 18, 639-40.

Stramer, B. M., Dunn, G. A., Davis, J. R., Mayor, R., 2013. Rediscovering contact inhibition in the embryo. J Microsc 251, 206–211.

Uesaka, T., Nagashimada, M., Yonemura, S., Enomoto, H., 2008. Diminished Ret expression compromises neuronal survival in the colon and causes intestinal aganglionosis in mice. J Clin Invest. 118, 1890-8.

Wallace, A. S. and Anderson, R. B., 2011. Genetic interactions and modifier genes in Hirschsprung's disease. World J. Gastroenterol. 17, 4937–4944.

Young, H. M., Hearn, C.J. Farlie, P.G. Canty, A.J. Thomas, P.Q. Newgreen, D.F., 2001. GDNF is a chemoattractant for enteric neural cells. Dev Biol 229, 503–516.

Young, H. M., Bergner, A. J., Simpson, M. J., McKeown, S. J., Hao, M. M., Anderson, C. R., Enomoto, H., 2014. Colonizing while migrating: how do individual enteric neural crest cells behave? BMC Biol. 12, 23.

Zhang, D., Brinas, I.M., Binder, B.J., Landman, K.A. & Newgreen, D.F., 2010. Neural crest regionalisation for enteric nervous system formation: Implications for Hirschsprung's disease and stem cell therapy. Dev. Biol. 339, 280–294.